



Biological nitrogen removal and metabolic characteristics of a novel aerobic denitrifying fungus *Hanseniaspora uvarum* strain KPL108

Haihan Zhang^{a,b,c,*}, Zhenfang Zhao^{a,b,c}, Pengliang Kang^{a,b,c}, Yue Wang^{a,b,c}, Ji Feng^{a,b,c}, Jingyu Jia^{a,b,c}, Zhonghui Zhang^{a,b,c}

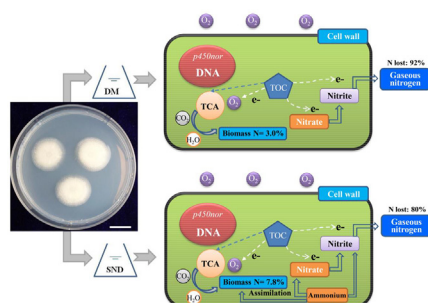
^a Shaanxi Key Laboratory of Environmental Engineering, Xi'an University of Architecture and Technology, Xi'an 710055, People's Republic of China

^b Key Laboratory of Northwest Water Resource, Environment and Ecology, MOE, Xi'an University of Architecture and Technology, Xi'an 710055, People's Republic of China

^c School of Environmental and Municipal Engineering, Institute of Environmental Microbial Technology, Xi'an University of Architecture and Technology, Xi'an 710055, People's Republic of China



GRAPHICAL ABSTRACT



ARTICLE INFO

Keywords:

Aerobic denitrifying fungus
Nitrogen removal
Metabolic characteristics
Response surface methodology
Hanseniaspora uvarum

ABSTRACT

A novel aerobic denitrifying fungal strain KPL108 was isolated from the sediment of Jinpen drinking water reservoir and identified as *Hanseniaspora uvarum*. Strain KPL108 removed 99% of nitrate without nitrite accumulation under aerobic conditions, while the total organic carbon removal efficiency was 93%. KPL108 expressed fungal specific denitrifying gene *p450nor*. Nitrogen balance exhibited that approximately 92% of the initial nitrate was removed as gaseous products. Based on ¹³C-isotope labeling tracer, pentose phosphate pathway and tricarboxylic acid cycle were highly active in intracellular central carbon metabolism of strain KPL108. Response surface methodology revealed that the maximum total nitrogen removal efficiency occurred with the optimized parameters: C/N ratio of 6.4, pH of 8.2, 28.5 °C and 109.7 rpm. Collectively, the results from the present study indicate that strain KPL108 has aerobic denitrification ability, which has a great potential application for nitrogenous wastewater treatment.

1. Introduction

With the fast development of global urbanization and extensive

fertilizer utilization activities, a large amount of nitrogen pollutants were discharged into diverse water bodies such as lakes, reservoirs and rivers (Carpenter et al., 1998). Nitrogen (N) pollution has created

* Corresponding author at: School of Environmental and Municipal Engineering, Institute of Environmental Microbial Technology, Xi'an University of Architecture and Technology, Xi'an 710055, People's Republic of China.

E-mail address: zhanghaihan@xauat.edu.cn (H. Zhang).

<https://doi.org/10.1016/j.biortech.2018.07.073>

Received 10 June 2018; Received in revised form 12 July 2018; Accepted 14 July 2018

0960-8524/ © 2018 Elsevier Ltd. All rights reserved.

several challenging environmental issues and public health problems (Camargo and Alonso, 2006). For instance, eutrophication, induced by heavy loading N, can cause toxic cyanobacterial bloom, which has serious influence on human health and aquatic organism development (Smith et al., 1999). Up to now, conventional treatment techniques focused on removing N are a combination of physico-chemical and biological processes (Hiscock et al., 1991). Additionally, biological treatment has been recognized as an effective and economical way for the removal of nitrogenous substances in natural or engineering ecosystems (Henze, 1991; Li et al., 2015).

Conventional denitrification processes refer to the conversion of nitrate (NO_3^- -N) or nitrite (NO_2^- -N) to gaseous nitrogen compounds by microorganisms exposed to anaerobic environments (Hiscock et al., 1991). In the past few decades, aerobic denitrifiers had attracted great attentions, which were continually isolated from activated sludge (Guo et al., 2016), marine sediment (Duan et al., 2015), drinking water reservoir sediment (Huang et al., 2015), urban lake (Kang et al., 2018), river biofilm (Lv et al., 2017) and membrane bioreactor (Zhao et al., 2010). Compared with the intensive studies focused on exploring the aerobic denitrifying bacterial strains such as *Enterobacter cloacae* HNR (Guo et al., 2016), *Vibrio diabolus* SF16 (Duan et al., 2015), and *Pseudomonas stutzeri* ZF31 (Huang et al., 2015), limited researches have highlighted the existence of fungi that are capable of performing denitrification under aerobic conditions (Zhou et al., 2001).

Fungi have several advantages over bacteria for N removal (Sankaran et al., 2010). One distinct advantage is that fungi have a higher capacity of organic matter decomposition due to the large amount of enzymes secreted from the mycelium. On the other hand, fungi have been demonstrated to have a higher denitrification rate than bacteria (Guest and Smith, 2002). In addition, fungal spores with complex cell walls, which enhance the fungal resistance to toxic compounds and harsh environments such as lower pH and higher temperature (Sankaran et al., 2010). Interestingly, Zhou et al. (2001) revealed that 80% of nitrate was recovered as the denitrification product N_2O by fungus *Fusarium oxysporum* strain MT-811. Denitrifying genes like *nirS* and *nirK* are related to bacteria (Kang et al., 2018). A novel fungal specific denitrifying gene named *p450nor* has been shown to drive the fungal denitrification process (Higgins et al., 2016). Moreover, Guest and Smith (2007) isolated 22 fungal strains and determined the potential for the development of fungal nitrogen removal technique for wastewater treatment. Currently, comprehensive exploration of the N removal potential of fungus is vital for developing advanced wastewater treatment technology.

Denitrifying process can simultaneously remove N and carbon (C), in which carbon source usually acts as electron donor and supplies energy element through intracellular various metabolic pathways (Hiscock et al., 1991; Marchant et al., 2017). Compared with massive literatures focused on exploring the nitrogen metabolic pathways (e.g., denitrifying function gene and nitrogen balance analysis), the central carbon metabolic (CCM) pathways of aerobic denitrifying microbe is still not well understood (Chen et al., 2016; Huang et al., 2015; Medhi et al., 2018). With the development of ^{13}C -stable isotope probing (SIP) used in metabolic engineering (Zamboni et al., 2005, 2009), the intracellular carbon metabolic pathways of aerobic denitrifying microbe can be comprehensively assessed. Unfortunately, no study was performed to delineate CCM pathways of aerobic denitrifying fungus using ^{13}C -stable isotope labeling approach.

To address this problem, the general aim of this work was to explore the characterization of a novel nitrifying-aerobic denitrifying fungal strain KPL108. The specific objectives were to: (1) identify the strain KPL108 using scanning electron microscopy combined with internal transcribed spacer (ITS) gene sequence; (2) determine the fungal specific denitrifying gene (*p450nor*); (3) examine the aerobic denitrification performance; (4) determine the intracellular CCM pathways by using ^{13}C -stable isotope labeling approach, and finally (5) to optimize the effects of process parameters, such as C/N ratio, pH, temperature,

and shaking speed on denitrification efficiency of strain KPL108 using the response surface methodology (RSM) model.

2. Material and methods

2.1. Fungal strain and media

In our previous studies, 123 strains were isolated from the sediments of the reservoirs (Jinpen, Zhouchun, Tangyu, Shibianyu and Lijiahe) and urban lakes (Kang et al., 2018; Zhang et al., 2018) in the past seven years. During the experiments, strain KPL108 has distinct colony and special morphological characteristics that have attracted our attention. Based on the preliminary results, strain KPL108 achieves efficient nitrate removal rate under aerobic conditions. Therefore, strain KPL108 was selected for further study. Denitrification medium (DM) per liter contained (pH = 7.2): 5 g of $\text{Na}_2\text{HPO}_4 \cdot 7\text{H}_2\text{O}$, 1.5 g of KH_2PO_4 , 0.1 g of $\text{MgSO}_4 \cdot 7\text{H}_2\text{O}$, 4.7 g of $\text{C}_4\text{H}_4\text{Na}_2\text{O}_4 \cdot 6\text{H}_2\text{O}$, 1.0 g of KNO_3 and 2 mL of trace element solution (Kang et al., 2018). In addition, simultaneous nitrification and denitrification (SND) medium per liter contained (pH = 7.2): 5 g of $\text{Na}_2\text{HPO}_4 \cdot 7\text{H}_2\text{O}$, 1.5 g of KH_2PO_4 , 0.1 g of $\text{MgSO}_4 \cdot 7\text{H}_2\text{O}$, 4.7 g of $\text{C}_4\text{H}_4\text{Na}_2\text{O}_4 \cdot 6\text{H}_2\text{O}$, 0.3 g of NH_4Cl , 1.0 g of KNO_3 and 2 mL of trace element solution (Kang et al., 2018). All media were autoclaved at 121 °C for 30 min.

2.2. Identification of the strain KPL108 and fungal denitrifying gene

To identify the strain KPL108, scanning electronic microscopy combined with internal transcribed spacer (ITS) gene sequencing techniques were performed. The morphological characteristics of strain KPL108 were measured using a scanning electron microscope (JSM-5800, Hitachi, Tokyo, Japan) as described previously (Kang et al., 2018). DNA was extracted using the DNA isolation kit according to the manufacturer's instructions. The ITS gene was amplified using primers ITS1 and ITS4 (Chhipa and Kaushik, 2017). In addition, the primers for *p450nor* gene were *p450nor394F* and *p450nor809R* (Higgins et al., 2016). The detailed information about the polymerase chain reaction (PCR) reactions and programs are listed in the Supplementary material. The PCR product of ITS gene was purified and sequenced by the Sanger method using ABI3730-XL sequencer (Applied Biosystems, USA). The ITS sequence was deposited in NCBI database with accession no. MG890280. A phylogenetic tree was carried out by MEGA (version 5.05) (Li et al., 2015).

2.3. Nitrifying-denitrifying capacity determination

To determine the nitrifying-denitrifying performance, the fungal suspension (24 mL) ($\text{OD} = 0.3$) was inoculated into 160 mL of DM and SND media using a 250-mL flask. All inoculated flasks were covered with gas permeable seals to allow air exchange, and cultivated aerobically with 130 rpm at 30 °C (Huang et al., 2015). The average dissolved oxygen (DO) concentration in the liquid medium was 6.3 ± 0.8 mg/L. The medium without inoculation was used as control. Samples were collected from flasks at 3 h intervals, with the optical density measured at 600 nm (OD_{600}) using a UVmini-1240 spectrophotometer (Shimadzu, Japan) (Zhou et al., 2001). The concentrations of ammonium (NH_4^+ -N), nitrate (NO_3^- -N), nitrite (NO_2^- -N), total organic carbon (TOC) and total nitrogen (TN) were also measured by the standard method (APHA, 1998).

2.4. Nitrogen balance analysis

To analyze the nitrogen balance of strain KPL108, the culture solutions were collected at 48 h, sonicated by a Scientz-IID ultrasonic cell disruption system (Ningbo, China), and used to determine the final TN concentration, which includes intracellular nitrogen (Zhao et al., 2010; Huang et al., 2015; Guo et al., 2016). After centrifugation for 10 min at

8000 rpm, the supernatants were filtered using 0.22- μ m membrane filters. The filtrates were used for determining the final soluble TN, NH_4^+ -N, NO_2^- -N and NO_3^- -N concentrations (Huang et al., 2015; Duan et al., 2015).

2.5. ^{13}C -isotope labeling central carbon metabolic pathways

To explore the intracellular CCM pathways, ^{13}C -isotope labeling technique was used. According to previous reports and protocol (Zamboni et al., 2009; Alagesan, et al., 2018), strain KPL108 (OD₆₀₀ = 0.4, 3% v/v) were inoculated into the flask with modified SND liquid medium, in which the carbon source of $\text{C}_4\text{H}_9\text{Na}_2\text{O}_4\cdot 6\text{H}_2\text{O}$ was replaced by labeled (1, 2- ^{13}C) glucose. The cells were cultivated aerobically with 130 rpm at 30 °C. At log phase of growth, 10 mL of culture solution was harvested and centrifuged for 10 min at 10,000 g. Approximately 30 mg of the pellet sample was mixed with 2 mL of HCl (6 M), and hydrolyzed the cell proteins into amino acids at 100 °C for 24 h. Amino acids were derivatized at 85 °C for 1 h, and then determined by gas chromatography-mass spectrometry as described previously (Zamboni et al., 2009). According to the retention times of amino acids including alanine, glycine, leucine, serine, phenylalanine, aspartate, glutamate, histidine, and tyrosine, etc. The CCM pathways were calculated and generated by metabolic flux analysis using MATLAB software packages (version 2012, Mathworks, Inc., Massachusetts) as described by Zamboni et al. (2005, 2009).

2.6. Optimization of the denitrification parameters

To assess the optimization of the denitrification condition, response surface methodology (RSM) combined with the Box-Behnken design (BBD) were employed for modeling the effects of independent variables, including C/N ratio, pH, temperature and shaking speed on denitrification efficiency (response) of the strain KPL108 (Huang et al., 2015). In total, 29 runs were carried out to optimize the four variables. Experimental ranges and levels of the independent variables for RSM and three-level-four-factor design matrix, the corresponding experimental and predicted responses of aerobic denitrification efficiency were summarized in Tables 1 and 2. Response surface (3D) and corresponding contour (2D) plots were generated from the models. The optimum values of the variables were calculated from the response surface (Design Expert software, version 7.1.5, Minneapolis, USA).

3. Results and discussion

3.1. Strain KPL108 identification and *p450nor* amplification

The diameter of white colony was approximately 2–3 cm after two weeks cultivation under aerobic conditions on DM medium plate. The colony surface was smooth, slightly raised at the center. The scanning electron microscope image allowed us to exhibit the structures of pseudohyphae and spores with more detail, which had a diameter of 0.5–1 μ m. The spores have subequatorial ledge, sometimes warty, which were around the pseudohyphae. This is consistent with previous

Table 1

Experimental ranges and levels of the independent variables for response surface methodology (RSM) model.

Variables	Symbols	Real values of coded levels ^a		
		–1	0	1
C/N ratio	X_1	1	6	11
Shaking speed (r/min)	X_2	0	65	130
Temperature (°C)	X_3	10	20	30
Initial pH	X_4	5	7	9

^a Low level (–1), center level (0), and high level (+1).

Table 2

Box-Behnken design matrix, corresponding experimental and predicted responses of aerobic denitrification efficiency as affected by C/N ratio, shaking speed, temperature, and pH.

Run	C/N ratio (variable: X_1)	Shaking speed (r/min) (variable: X_2)	Temperature (°C) (variable: X_3)	Initial pH (variable: X_4)	TN removal efficiency (%) (Response)
1	1(–1) ^a	0(–1)	20(0)	7(0)	54.21
2	1(–1)	65(0)	10(–1)	7(0)	35.15
3	1(–1)	65(0)	20(0)	5(–1)	13.21
4	1(–1)	65(0)	20(0)	9(+1)	42.86
5	1(–1)	65(0)	30(+1)	7(0)	61.10
6	1(–1)	130(+1)	20(0)	7(0)	53.43
7	6(0)	0(–1)	10(–1)	7(0)	52.14
8	6(0)	0(–1)	20(0)	5(–1)	21.89
9	6(0)	0(–1)	20(0)	9(+1)	76.00
10	6(0)	0(–1)	30(+1)	7(0)	87.21
11	6(0)	65(0)	10(–1)	5(–1)	8.15
12	6(0)	65(0)	10(–1)	9(+1)	34.10
13	6(0)	65(0)	20(0)	7(0)	74.43
14	6(0)	65(0)	20(0)	7(0)	75.86
15	6(0)	65(0)	20(0)	7(0)	76.12
16	6(0)	65(0)	20(0)	7(0)	78.10
17	6(0)	65(0)	20(0)	7(0)	76.54
18	6(0)	65(0)	30(+1)	5(–1)	20.57
19	6(0)	65(0)	30(+1)	9(+1)	92.87
20	6(0)	130(+1)	10(–1)	7(0)	47.91
21	6(0)	130(+1)	20(0)	5(–1)	17.26
22	6(0)	130(+1)	20(0)	9(+1)	77.21
23	6(0)	130(+1)	30(+1)	7(0)	86.88
24	11(+1)	0(–1)	20(0)	7(0)	81.10
25	11(+1)	65(0)	10(–1)	7(0)	52.20
26	11(+1)	65(0)	20(0)	5(–1)	15.36
27	11(+1)	65(0)	20(0)	9(+1)	86.50
28	11(+1)	65(0)	30(+1)	7(0)	91.50
29	11(+1)	130(+1)	20(0)	7(0)	79.24

^a The center point was replicated five times to estimate the experimental errors.

study carried out by Malandra et al. (2003), who determined the microbiology of a biological contactor for winery wastewater treatment and found that *H. uvarum* was able to form pseudohyphae. At the same time, the ITS sequence (406 bp) revealed that the strain KPL108 had a high similarity (99%) with the fungus, *H. uvarum* strain P43. Neighbor-joining analysis of fungal internal transcribed spacer (ITS) gene sequence of the strain KPL108 was shown in Fig. 1. The morphological characteristics and the ITS sequence identification indicate that the strain KPL108 affiliates *Hanseniaspora uvarum*. Previously, Tsuruta et al. (1998) found that *H. guilliermondii* could convert nitrite into N_2O due to nitric oxide reductase cytochrome P450nor received electrons from nicotinamide adenine dinucleotide (NADH). In this work, the fungal denitrifying gene *p450nor* was amplified from KPL108, and shown in Supplementary material. This is consistent with the previous work conducted by Higgins et al. (2016), who observed *p450nor* gene in 23 fungal strains, and these fungal species performed aerobic denitrification.

3.2. Nitrogen removal and balance

Fig. 2(A) shows the aerobic denitrification ability of strain KPL108. A significant decrease of NO_3^- -N was observed for strain KPL108 between 9 h and 12 h. After 35 h of cultivation, the NO_3^- -N concentration decreased from 138 mg/L to 1.07 mg/L, while 99.22% of NO_3^- -N was removed by strain KPL108 (Fig. 2A). Pires et al. (2017) isolated *Hanseniaspora uvarum* strain from a coffee processing wastewater treatment plant, and found that *H. uvarum* played vital roles in nitrogen and carbon oxygen demand removal processes. The present result is consistent with a previous related fungus report by Zhou et al. (2001),

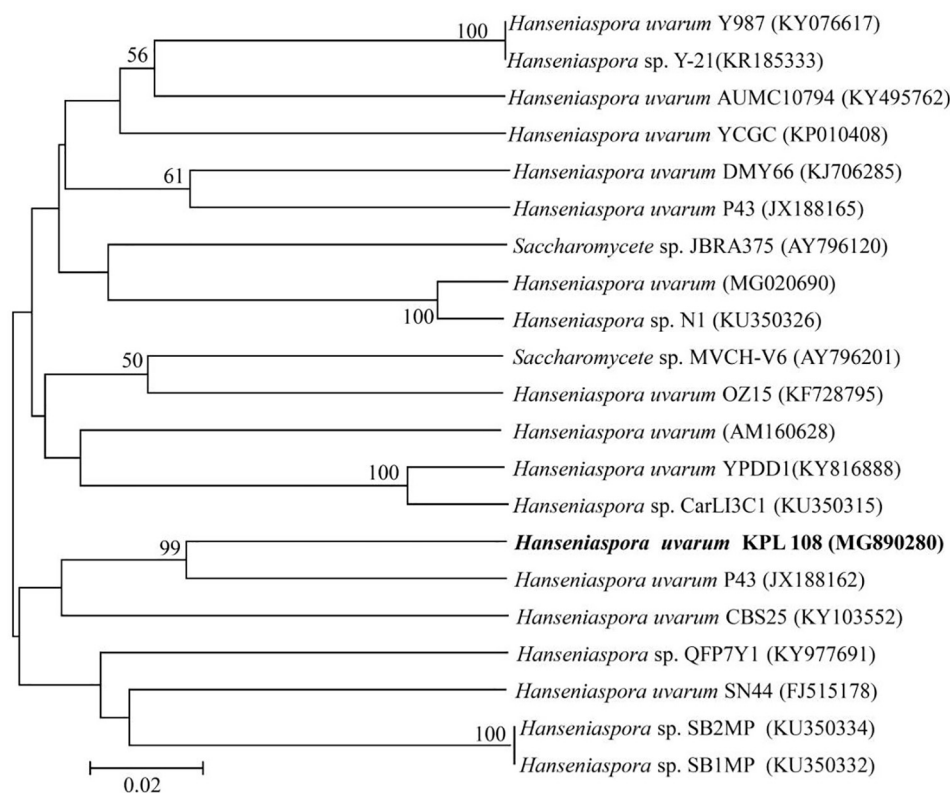


Fig. 1. Neighbor-joining analysis of fungal internal transcribed spacer (ITS) gene sequence of the strain KPL108. References strains were selected from GenBank based on ITS gene.

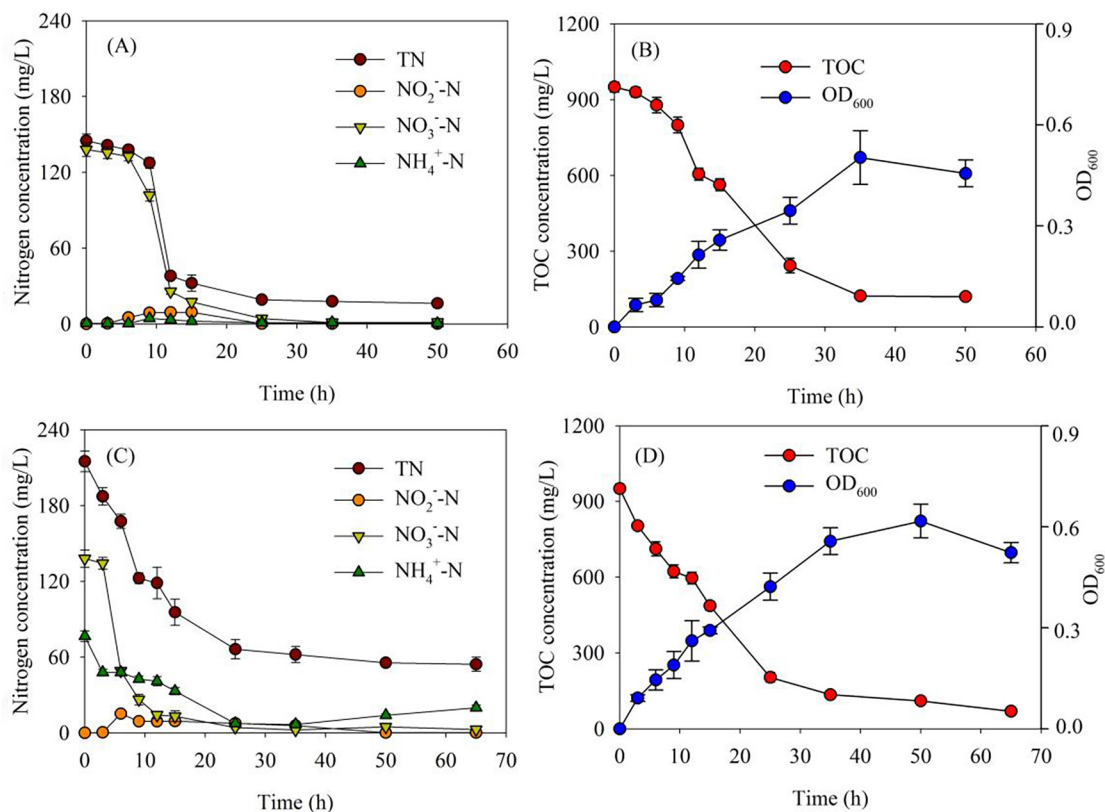


Fig. 2. (A) Aerobic denitrification performance, (B) growth curve and total organic carbon (TOC) removal of the strain KPL108, (C) Simultaneous nitrification-aerobic denitrification performance, (D) growth curve and total organic carbon (TOC) removal of the strain KPL108.

which showed that *Fusarium oxysporum* MT-811 could convert NO_3^- -N to N_2O under O_2 supply. Moreover, fungal specific *p450nor* gene was detected and revealed that *p450nor* could derive the denitrification process of fungal denitrifiers (Higgins et al., 2016). The highest NO_3^- -N removal rate was 9.37 mg NO_3^- -N/L/h, which was higher than several aerobic denitrifying bacteria such as 2.83 mg NO_3^- -N/L/h for *Vibrio diabolus* strain SF16 (Duan et al., 2015), 8.78 mg NO_3^- -N/L/h for *Pseudomonas stutzeri* strain ZF31 (Huang et al., 2015) and 3.1 mg NO_3^- -N/L/h for *Rhodococcus* sp. strain CPZ24 (Chen et al., 2012). At the same time, the NO_2^- -N concentrations increased gradually between 15 h and 25 h before decreasing to 0.03 mg/L at 25 h. Fungal cell growth increased steadily, which reached 0.5 at 35 h. The growth curve equation was $Y = 0.0024 X^2 + 0.0389 X - 0.0415$ ($r^2 = 0.961$). Simultaneously, TOC concentration had a significant negative relationship with fungal biomass during cultural periods (Pearson's correlation, $r = -0.986$, $P < 0.001$, $n = 9$). Strain KPL108 removed 87% of TOC under aerobic conditions (Fig. 2B), while the TOC removal rate was 28.28 mg/L/h. Interestingly, the TOC removal efficiency was higher than that of the aerobic denitrifying bacterium, *Pseudomonas stutzeri* strain ZF31 with 74%, which was isolated from Zhoucun drinking water reservoir, Shandong province, China (Huang et al., 2015).

Furthermore, strain KPL108 also displays relative high simultaneous nitrifying-denitrifying capability. As shown in Fig. 2(C and D), after 25 h of cultivation, the NH_4^+ -N concentration decreased from 76.5 mg/L to 7.39 mg/L, while the NH_4^+ -N removal rate was 2.76 mg NH_4^+ -N/L/h. Apparently, the growth curve equation was $Y = -0.0007 X^2 + 0.0758 X - 0.079$ ($r^2 = 0.943$). The growth curves of strain KPL108 were similar in the DM and SND media, while the fungal biomass (OD_{600}) reached 0.62 at 50 h. This fungal biomass was also significantly negative correlated with TOC concentration (Pearson's correlation, $r = -0.984$, $P < 0.001$, $n = 9$) (Fig. 2D). Interestingly, 81% of NO_3^- -N was removed at 9 h cultivation, which was approximately 3.12-fold higher than that of the DM medium. This result is consistent with a previous report, which suggested that the addition of ammonium could increase the aerobic denitrification efficiency (Sun et al., 2017).

In the present work, the removal efficiencies of NH_4^+ -N and TOC were 74% and 93%, respectively. At the end of experiment, approximately 60 mg/L of TN was left in the medium. It is clearly showed that the TN removal efficiency was 75%. The most important reason may be that with the extension of cultural periods, the liquid medium conditions are not suitable for the cell growth (e.g., depletion of nutrition). Interestingly, compared to other previous reports, strain KPL108 could be a better aerobic denitrifier candidate compared to the reported bacterial strains for the simultaneous removal of NH_4^+ -N, NO_3^- -N and TOC (Li et al., 2015; Shi et al., 2013). Moreover, *Hanseniaspora uvarum* strain MEA5 was isolated previously from a rotating biological contactor treating winery wastewater by Malandra et al. (2003), who demonstrated that strain MEA5 reduced the 95% of chemical oxygen demand (COD) under aerated conditions. As shown in Table 4, the nitrogen balance indicated that approximately 92% and 80% of nitrogen was lost as gaseous products within DM and SND media environments, respectively. Moreover, 3.0% and 7.8% of the removed nitrogen were converted to biomass (Table 4). The biomass of the intracellular nitrogen was higher when the strain KPL108 was cultivated in the SND medium with ammonium. It is confirmed that strain KPL108 has the capacity for ammonium nitrogen assimilation. This result is consistent with a previous study carried out by Sun et al. (2017), who found that ammonium was utilized through assimilation rather than heterotrophic nitrification during aerobic denitrification of *Pseudomonas stutzeri* T13.

3.3. Central carbon metabolic pathways

To experimentally identify complex intracellular metabolic networks, strain KPL108 was fed with labeled ^{13}C -glucose as sole carbon source. The growth curve was shown in the Supplementary material. Based on the ^{13}C tracer data, protein derived amino acids were used to

Table 3

Analysis of variance (ANOVA) for response surface quadratic model (Y^a).

Sources	Mean Square	F-value	P-value	Statistics
Model ^b	1451.42	307.40	< 0.0001	Significant
X_1	1774.87	375.91	< 0.0001	Significant
X_2	9.40	1.99	0.1801	NS
X_3	3691.82	781.90	< 0.0001	Significant
X_4	8169.30	1730.21	< 0.0001	Significant
X_1X_2	0.29	0.062	0.8073	NS
X_1X_3	44.56	9.44	0.0083	Significant
X_1X_4	430.36	91.15	< 0.0001	Significant
X_2X_3	3.80	0.81	0.3847	NS
X_2X_4	8.53	1.81	0.2004	NS
X_3X_4	537.08	113.75	< 0.0001	Significant
X_1^2	473.21	100.22	< 0.0001	Significant
X_2^2	0.085	0.018	0.9667	NS
X_3^2	420.47	89.05	< 0.0001	Significant
X_4^2	5278.36	1117.92	< 0.0001	Significant
Residual error	4.72			
Lack of fit	5.91	3.39	0.1254	NS
Pure error	1.74			
Total	1451.42			

NS: not significant.

^a The results were generated from the Design Expert software (version 8.0).

^b X_1 is C/N ratio. X_2 is shaking speed. X_3 is temperature. X_4 is pH.

assess the estimated metabolic fluxes distribution. Most alanine was non-labeled, therefore, pentose phosphate (PP) pathway was active. Moreover, 76% and 23% of the total carbon uptake were metabolized by glycolysis and PP pathways, revealing that less carbon flux went through the PP pathway (Fig. 3). A high anaplerosis flux via phosphoenolpyruvate carboxylase (132 ± 2) was observed. However, Entner–Doudoroff (ED) pathway was not found. The CCM pathways of strain KPL108 were shown in Fig. 3. ^{13}C -labeled metabolic flux analysis (MFA) revealed that Tricarboxylic acid (TCA) cycle conferred in carbon and energy metabolism in strain KPL108. The total flux through citrate was 63%. TCA cycle was the main energy (e.g., ATP) and nicotinamide adenine dinucleotide (NADH) producing pathway, which improved the metabolic of converting nitrate to nitrogen gas (N_2) using electron from carbon metabolic pathways. The result is, in general, consistent with the reports by Marchant et al. (2017) and Kawakami et al. (2010), who suggested that denitrification occurred at high O_2 concentrations, and carbon source used as electron donor for diverse enzymes in the aerobic respiration of denitrification process. During the simultaneous nitrification-aerobic denitrification, carbon source was oxidized to carbon dioxide (CO_2) and converted to biomass via a complete tricarboxylic acid cycle. Strikingly, we found that the fungal biomass was also significantly negatively correlated with total organic carbon concentration. To confirm the pathways, the genome sequence of *Hanseniaspora uvarum* AWRI3580 and 3410 protein coding genes were reported by Sterner et al. (2016) and Langenberg et al. (2017).

In PP and TCA pathways, several enzymes (e.g., NADH dehydrogenase and pyruvate kinase) play critical roles in driving biochemical reactions. Recently, Langenberg et al. (2017) observed that strain DSM2768 had higher pyruvate kinase and decarboxylase activities when grown in the medium with glucose as sole carbon source. Interestingly, under anaerobic conditions, higher pyruvate kinase activity of *H. uvarum* was observed during glucose consumption (Langenberg et al., 2017). Similarly, a denitrifying bacterium, *Pseudomonas denitrificans*, converted 96% carbon into bacterial biomass and CO_2 under aerobic bath culture conditions (Koike and Hattori, 1975). CO_2 was produced from pyruvate (PRY) to Acetyl-CoA (Ac CoA), from isocitrate (ICT) to α -ketoglutarate (AKG), from malate (MAL) to oxaloacetate (OAA) (Fig. 3). Under aerobic conditions, the physiology of *Hanseniaspora uvarum* strain K5 was determined by Venturin et al. (1995), who found that glucose was aerobically metabolized in biomass and CO_2 , and strain K5 metabolized pyruvate using pyruvate

Table 4
Nitrogen balance of the strain KPL108 under aerobic conditions (unit: mg).

Substance	Initial TN	Final nitrogen				Intracellular N	N lost
		NO ₃ [−] -N	NO ₂ [−] -N	NH ₄ ⁺ -N	Organic-N		
Nitrogen ^a	25.39 ± 0.64	0.64 ± 0.22	0.01 ± 0.00	0.05 ± 0.02	0.57 ± 0.01	0.77 ± 0.28	23.35 ± 0.32
Nitrogen ^b	39.56 ± 1.40	0.18 ± 0.02	0.01 ± 0.00	1.87 ± 0.25	2.90 ± 0.43	3.09 ± 0.29	31.51 ± 0.43

Values are means ± standard deviation (SD) (n = 3).
TN: total nitrogen.
^a Nitrate as sole nitrogen source for aerobic denitrifying performance determination.
^b Nitrate and ammonium as nitrogen sources for simultaneous nitrifying-aerobic denitrifying performance determination.

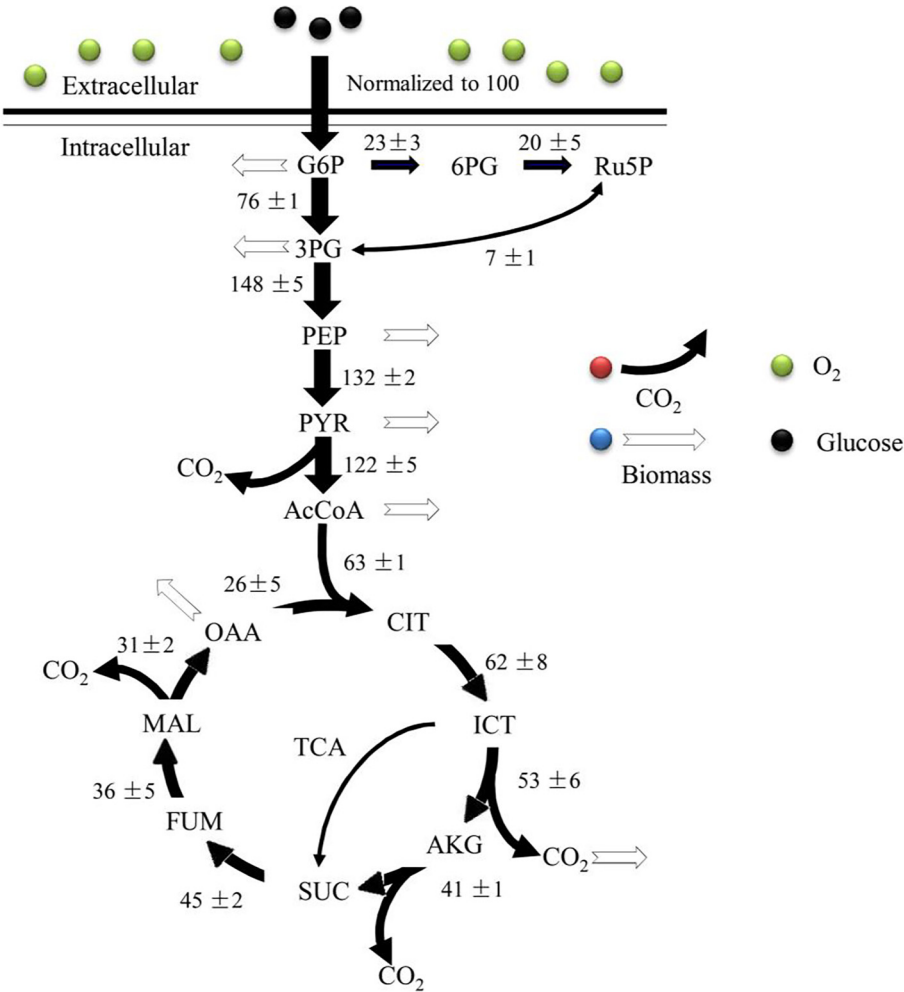


Fig. 3. The central carbon metabolic (CCM) pathways of the strain KPL108 based on ¹³C-glucose isotope labeling. G6P: glucose-6-phosphate, 6PG: 6-phosphogluconate, Ru5P: ribulose 5-phosphate, 3PG: 3-phosphoglycerate, PEP: phosphoenolpyruvate, PYR: pyruvate, AcCoA: Acetyl-CoA, OAA: oxaloacetate, CIT: citrate, ICT: isocitrate, AKG: α-ketoglutarate, SUC: succinate, FUM: fumarate, MAL: malate. TCA: tricarboxylic acid cycle. The estimated fluxes in the map were proportions of the relative rates normalized to glucose uptake rates (100%).

dehydrogenase. Moreover, [Albergaria et al. \(2003\)](#) suggested that *Hanseniaspora guilliermondii* converted glucose into glycerol, biomass and CO₂ under aerobic glucose continuous culture conditions. Unfortunately, no genome of *Hanseniaspora uvarum* was deposited in Kyoto Encyclopedia of Genes and Genomes (KEGG) database, but the first genome of *Hanseniaspora vineae* strain T02/19AF was reported by [Giorello et al. \(2014\)](#), who demonstrated that 128 genes related to TCA cycle and PP pathway. During these pathways, NADH/FADH₂, NADPH and ATP were produced and consumed. Importantly, based on the electron transport chain, electrons can be transferred from NADH to nitrite reductase due to O₂ and nitrate are equally electron acceptors ([Chen and Strous, 2013](#)). Overall, novel insights into the CCM pathways

presented here will help environmental engineer to answer the fundamental question of how this fungus achieves aerobic denitrifying ability, and open up alternative strategies like genetically engineered this strain (e.g., function gene mutants from synthetic biology) for improved nitrogen and carbon simultaneous removal performance.

3.4. Box–Behnken design for optimizing the parameters

Based on the response surface methodology (RSM) with a three-level-four-factor Box–Behnken experimental design, the quadratic model regression equation generated by multiple regression analysis ($R^2 = 0.997$) is as follows:

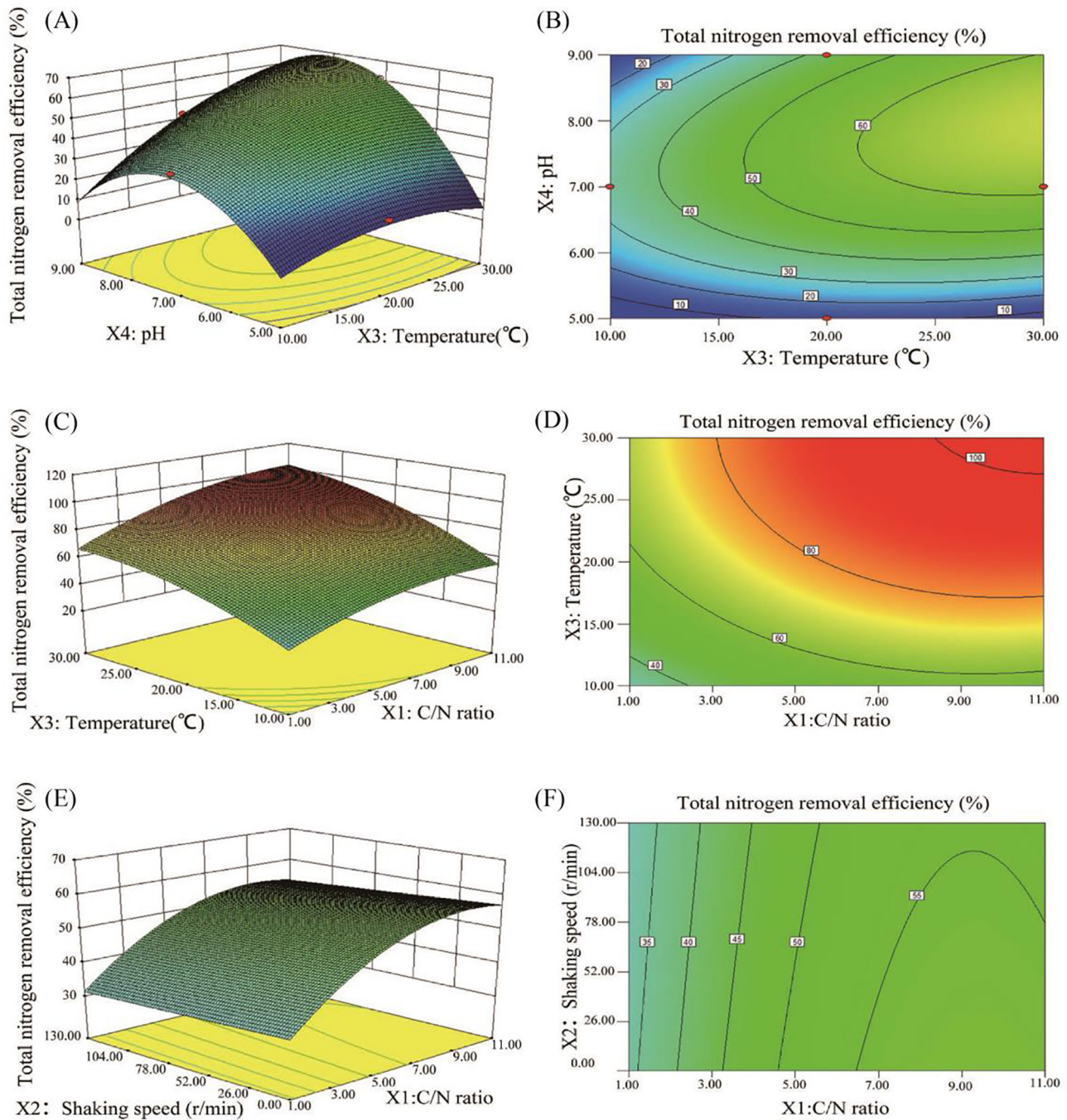


Fig. 4. Response surface (3D) and corresponding contour (2D) plots for total nitrogen removal efficiency (%) of the strain KPL108: (A and B) effects of pH and temperature on total nitrogen removal efficiency (%), (C and D) effects of temperature and C/N ratio on total nitrogen removal efficiency (%), (E and F) effects of shaking speed and C/N ratio on total nitrogen removal efficiency (%).

$$Y(\%) = 76.21 + 12.16X_1 - 0.89X_2 + 17.54X_3 + 26.09X_4 - 0.27X_1X_2 + 3.34X_1X_3 + 10.37X_1X_4 + 0.98X_2X_3 + 1.46X_2X_4 + 11.59X_3X_4 - 8.54X_1^2 + 0.036X_2^2 - 8.05X_3^2 - 28.53X_4^2$$

where, Y is the response model (TN removal efficiency, %). X_1 , X_2 , X_3 and X_4 are the coded values of C/N ratio, shaking speed, temperature and initial pH, respectively. The F -value of model was 307.40. The P -value of the lack of fit ($P = 0.1254$) and the model ($P < 0.001$) revealed that the obtained experimental data exhibited a good fit with this model (Table 3). The value of the determination coefficient ($R^2 = 0.997$) indicated that 99.68% of the total variable could be explained by the model.

To further visualize these relationships, response surfaces were also plotted to show the effects of the tested factors on TN removal of strain KPL108. Fig. 4 displayed the response surface and contours lines of the TN removal efficiency affected by temperature and pH, which suggested that the positive effect of increased pH on TN removal efficiency was more pronounced than temperature (Fig. 4A and B). Analogously, the response surface and contours of the TN removal were shown in Fig. 4(C and D) as a function of C/N ratio and temperature variables. The interactions between C/N ratio and temperature were significant ($P = 0.0083$) (Table 3). The TN removal efficiency was increased significantly with an increasing of C/N ratio and temperature. As illustrated in Fig. 4, the 3D surface plot (Fig. 4E) and 2D (Fig. 4F) contour

plot for the TN removal model showed that the maximum TN removal was occurred with the C/N ratio of 9. However, the interactions between C/N ratio and shaking speed were not significant ($P = 0.8073$). Together, the order of importance of the four variables with respect to denitrification efficiency was $\text{pH} > \text{temperature} > \text{C/N ratio} > \text{shaking speed}$. Previous studies also demonstrated that denitrifying efficiency was regulated mainly by pH (Yan et al., 2016; Qu et al., 2015), temperature (Yao et al., 2013) and C/N ratio (Ren et al., 2014), and O_2 concentrations (Ji et al., 2014; Marchant et al., 2017).

In the current study, the mathematical model predicted that the maximum value of the TN removal efficiency was 98.75%. RSM based on BBD revealed that the maximum removal efficiency of TN occurred with conditions: C/N ratio of 6.4, 109.7 rpm, 28.5 °C and a pH of 8.2. The result is consisted with an aerobic denitrifying bacteria, *Pseudomonas stutzeri* strain ZF31 isolated from the sediment of Zhouchun drinking water reservoir, suggested that the maximum TN removal occurred with pH 8.2, a C/N ratio of 6.7, and temperature of 28 °C (Huang et al., 2015). Previous studies also have shown that the Box-Behnken design RSM is an effective strategy for modeling and optimizing multi-factor experiments to clarify how the single and interaction effects influence the denitrification efficiency of aerobic denitrifying microbe, such as *Raoultella* sp. strain sari0 (Yan et al., 2016), *Pseudomonas migulae* strain AN-1 (Qu et al., 2015), *Pseudomonas* strain T13 (Du et al., 2015), and for optimizing simultaneous pollution removal biological aerated filter (Hasan et al., 2011), as well as the removal of nitrate from wastewater treatment using *Pseudomonas stutzeri* in a bioreactor (Naik and Setty, 2014). All together, although the novel results can be drawn in this study, to the best of our knowledge, the present study provides the first insight into the CCM pathways associated with an efficient aerobic denitrifying fungus. Based on the principles of synthetic biology, to enhance these metabolic pathways of the strain KPL108 for nitrogen and carbon removal, the whole genome sequence, western blot, intracellular proteomics expression (e.g. key enzyme activity) combined with genome-scale ^{13}C -MFA should be further explored. Thus, these results will set the foundation knowledge for development of novel nitrogenous wastewater treatment technology by using aerobic denitrifying fungi or genetic engineering strains generated by synthetic biology.

4. Conclusions

Fungal strain KPL108 was identified as *Hanseniaspora uvarum*, and the fungal specific denitrifying gene (*p450nor*) was detected. KPL108 removed nitrate and ammonium at rates of 9.37 mg/L/h and 2.76 mg/L/h, respectively. Approximately 92% of the nitrate was converted into gaseous products. PP pathway and TCA cycle were the active intracellular CCM pathways. The RSM model revealed that the maximum removal of TN occurred with C/N ratio of 6.4, pH of 8.2, 28.5 °C and 109.7 rpm. These results suggest that strain KPL108 can be a suitable candidate for nitrogenous wastewater treatment.

Acknowledgments

This work was supported by the International Science and Technology Cooperation Program (2018KW-011), the National Key Research and Development Program of China (2016YFC0400706), the grants from “Young Outstanding Talents” in University of Shaanxi Province, and “Yanta Outstanding Youth Scholar” in Xi'an University of Architecture and Technology, China. All authors appreciate the useful comments from three anonymous reviewers to enhance the manuscript.

Conflict of interest

The authors declare that they have no competing interests.

Appendix A. Supplementary data

Supplementary data associated with this article can be found, in the online version, at <https://doi.org/10.1016/j.biortech.2018.07.073>.

References

- Alagesan, S., Minton, N.P., Malys, N., 2018. ^{13}C -assisted metabolic flux analysis to investigate heterotrophic and mixotrophic metabolism in *Cupriavidus necator* H16. *Metabolomics* 14, 9.
- Albergaria, H., Torrao, A.R., Hogg, T., Girio, F.M., 2003. Physiological behavior of *Hanseniaspora guilliermondii* in aerobic glucose-limited continuous cultures. *FEMS Yeast Res.* 3, 211–216.
- APHA, 1998. Standard methods for the examination of water and wastewater. American Public Health Association, Washington, DC, USA.
- Camargo, J.A., Alonso, A., 2006. Ecological and toxicological effects of inorganic nitrogen pollution in aquatic ecosystems: a global assessment. *Environ. Int.* 32, 831–849.
- Carpenter, S.R., Caraco, N.F., Correll, D.L., Howarth, R.W., Sharpley, A.N., Smith, V.H., 1998. Nonpoint pollution of surface waters with phosphorus and nitrogen. *Ecol. Appl.* 8, 559–568.
- Chen, J., Gu, S.Y., Hao, H.H., Chen, J.M., 2016. Characteristics and metabolic pathway of *Alcaligenes* sp. TB for simultaneous heterotrophic nitrification-aerobic denitrification. *Appl. Microbiol. Biotechnol.* 100 (22), 9787–9794.
- Chen, P.Z., Li, J., Li, Q.X., Wang, Y.C., Li, S.P., Ren, T.Z., Wang, L.G., 2012. Simultaneous heterotrophic nitrification and aerobic denitrification by bacterium *Rhodococcus* sp. CPZ24. *Bioresour. Technol.* 116, 266–270.
- Chen, J.W., Strous, M., 2013. Denitrification and aerobic respiration, hybrid electron transport chains and co-evolution. *BBA-Bioenergetics* 1827 (2), 136–144.
- Chhipa, H., Kaushik, N., 2017. Fungal and bacterial diversity isolated from *Aquilaria malaccensis* tree and soil, induces agarospore formation within 3 months after artificial infection. *Front. Microbiol.* 8, 1286.
- Du, C., Cui, C.W., Deng, F.X., Li, A., Ma, F., 2015. Identification of a highly efficient aerobic denitrifier and denitrification optimization using response surface method. *Microbiol. China.* 42 (5), 872–882.
- Duan, J.M., Fang, H.D., Su, B., Chen, J.F., Lin, J.M., 2015. Characterization of a halophilic heterotrophic nitrification-aerobic denitrification bacterium and its application on treatment of saline wastewater. *Bioresour. Technol.* 179, 421–428.
- Giorrello, F.M., Berná, L., Greif, G., Camesasca, L., Salzman, V., Medina, K., Robello, C., Gaggero, C., Aguilar, P.S., Carrau, F., 2014. Genome sequence of the native apiculate wine yeast *Hanseniaspora vineae* T02/19AF. *Genome Announc.* 2 (3), e00530–14.
- Guest, R.K., Smith, D.W., 2002. A potential new role for fungi in a wastewater MBR biological nitrogen reduction system. *J. Environ. Eng. Sci.* 6, 433–437.
- Guest, R.K., Smith, D.W., 2007. Isolation and screening of fungi to determine potential for ammonia nitrogen treatment in wastewater. *J. Environ. Eng. Sci.* 6, 209–217.
- Guo, L.J., Zhao, B., An, Q., Tian, M., 2016. Characteristics of a novel aerobic denitrifying bacterium, *Enterobacter cloacae* strain HNR. *Appl. Biochem. Biotech.* 178, 947–959.
- Hasan, H.A., Abdullah, S.R.S., Kamarudin, S.K., Kofli, N.T., 2011. Response surface methodology for optimization of simultaneous COD, NH_4^+ -N and Mn^{2+} removal from drinking water by biological aerated filter. *Desalination.* 275, 50–61.
- Henze, M., 1991. Capabilities of biological nitrogen removal processes from wastewater. *Water Sci. Technol.* 23, 669–679.
- Higgins, S.A., Welsh, A., Orellana, L.H., Konstantinidis, K.T., Chee-Sanford, J.C., Sanford, R.A., Schadt, C.W., Löffler, F.E., 2016. Detection and diversity of fungal nitric oxide reductase genes (*p450nor*) in agricultural soils. *Appl. Environ. Microbiol.* 82, 2919–2928.
- Hiscock, K.M., Lloyd, J.W., Lerner, D.N., 1991. Review of natural and artificial denitrification of groundwater. *Water Res.* 25, 1099–1111.
- Huang, T.L., Guo, L., Zhang, H.H., Su, J.F., Wen, G., Zhang, K., 2015. Nitrogen-removal efficiency of a novel aerobic denitrifying bacterium, *Pseudomonas stutzeri* strain ZF31, isolated from a drinking-water reservoir. *Bioresour. Technol.* 196, 209–216.
- Ji, B., Wang, H.Y., Yang, K., 2014. Tolerance of an aerobic denitrifier (*Pseudomonas stutzeri*) to high. *Biotechnol. Lett.* 36, 719–722.
- Kang, P.L., Zhang, H.H., Huang, T.L., Chen, S.N., Shang, P.L., Feng, J., Jia, J.Y., 2018. Denitrification characteristics and community structure of aerobic denitrifiers from lake and reservoir sediments. *Environ. Sci.* 5, 1–10.
- Kawakami, T., Kuroki, M., Ishii, M., Igarashi, Y., Arai, H., 2010. Differential relative abundance of multiple terminal oxidases for aerobic respiration in *Pseudomonas aeruginosa*. *Environ. Microbiol.* 12, 1399–1412.
- Koike, I., Hattori, A., 1975. Growth yield of a denitrifying bacterium, *Pseudomonas denitrificans*, under aerobic and denitrifying conditions. *J. Gen. Microbiol.* 88, 1–10.
- Langenberg, A.K., Bink, F.J., Wolff, L., Walter, S., von Wallbrunn, C., Grossmann, M., Heinisch, J.J., Schmitz, H.P., 2017. Glycolytic functions are conserved in the genome of the wine yeast *Hanseniaspora uvarum*, and pyruvate kinase limits its capacity for alcoholic fermentation. *Appl. Environ. Microbiol.* 83, e01580–17.
- Li, C.N., Yang, J.S., Wang, X., Wang, E.T., Li, B.Z., He, R.X., Yuan, H.L., 2015. Removal of nitrogen by heterotrophic nitrification-aerobic denitrification of a phosphate accumulating bacterium *Pseudomonas stutzeri* YG-24. *Bioresour. Technol.* 182, 18–25.
- Lv, P.Y., Luo, J.X., Zhuang, X.L., Zhang, D.Q., Huang, Z.B., Bai, Z.H., 2017. Diversity of culturable aerobic denitrifying bacteria in the sediment, water and biofilms in Liangshui River of Beijing. *China. Sci. Rep.* 7, 10032.
- Malandra, L., Wolfaardt, G., Zietsman, A., Viljoen-Bloom, M., 2003. Microbiology of a biological contactor for winery wastewater treatment. *Water Res.* 37 (17), 4125–4134.
- Marchant, H.K., Ahmerkamp, S., Lavik, G., Tegetmeyer, H.E., Graf, J., Klatt, J.M.,

- Holtappels, M., Walpersdorf, E., Kuypers, M.M.M., 2017. Denitrifying community in coastal sediments performs aerobic and anaerobic respiration simultaneously. *ISME J.* 11, 1799–1812.
- Medhi, K., Mishra, A., Thaku, I.S., 2018. Genome sequence of a heterotrophic nitrifier and aerobic denitrifier, *Paracoccus denitrificans* strain ISTOD1, isolated from wastewater. *Genome Announc.* 6 (15), e00210–18.
- Naik, S.S., Setty, Y.P., 2014. Optimization of parameters using response surface methodology and genetic algorithm for biological denitrification of wastewater. *Int. J. Environ. Sci. Technol.* 11, 823–830.
- Pires, J.F., Cardoso, L.S., Schwan, R.F., Silva, C.F., 2017. Diversity of microbiota found in coffee processing wastewater treatment plant. *World J. Microbiol. Biotechnol.* 33 (12), 211.
- Qu, D., Wang, C., Wang, Y.Y.F., Zhou, R., Ren, H.J., 2015. Heterotrophic nitrification and aerobic denitrification by a novel groundwater origin cold-adapted bacterium at low temperatures. *RSC Adv.* 5, 5149–5157.
- Ren, Y.X., Yang, L., Liang, X., 2014. The characteristics of a novel heterotrophic nitrifying and aerobic denitrifying bacterium, *Acinetobacter junii* YB. *Bioresour. Technol.* 171, 1–9.
- Sankaran, S., Khanal, S.K., Jasti, N., Jin, B., Pometto III, A.L., Van Leeuwen, J.H., 2010. Use of filamentous fungi for wastewater treatment and production of high value fungal byproducts: a review. *Crit. Rev. Env. Sci. Tec.* 40, 400–449.
- Shi, Z., Zhang, Y., Zhou, J.T., Chen, M.X., Wang, X.J., 2013. Biological removal of nitrate and ammonium under aerobic atmosphere by *Paracoccus versutus* LYM. *Bioresour. Technol.* 148, 144–148.
- Smith, V.H., Tilman, G.D., Nekola, J.C., 1999. Eutrophication: impacts of excess nutrient inputs on freshwater, marine, and terrestrial ecosystem. *Environ. Pollut.* 100, 179–196.
- Sternes, P.R., Lee, D., Kutyna, D.R., Borneman, A.R., 2016. Genome sequences of three species of *Hanseniaspora* isolated from spontaneous wine fermentations. *Genome Announc.* 4, e01287–16.
- Sun, Y.L., Feng, L., Li, A., Zhang, X.N., Yang, J.X., Ma, F., 2017. Ammonium assimilation: An important accessory during aerobic denitrification of *Pseudomonas stutzeri* T13. *Bioresour. Technol.* 234, 264–272.
- Tsuruta, S., Takaya, N., Zhang, L., Shoun, H., Kimura, K., Hamamoto, M., Nakase, T., 1998. Denitrification by yeasts and occurrence of cytochrome P450nor in *Trichosporon cutaneum*. *FEMS Microbiol. Lett.* 168, 105–110.
- Venturin, C., Boze, H., Moulin, G., Galzy, P., 1995. Glucose metabolism, enzymic analysis and product formation in chemostat culture of *Hanseniaspora uvarum*. *Yeast* 11, 327–336.
- Yan, W.Z., Hao, J., Sun, J.S., Shi, J.P., 2016. Isolation of *Raoultella* sp. sari01 and its heterotrophic nitrification-aerobic denitrification characteristics. *Environ. Sci.* 37, 2673–2680.
- Yao, S., Ni, J.R., Ma, T., Li, C., 2013. Heterotrophic nitrification and aerobic denitrification at low temperature by a newly isolated bacterium, *Acinetobacter* sp. HA2. *Bioresour. Technol.* 139, 80–86.
- Zamboni, N., Fischer, E., Sauer, U., 2005. FiatFlux – a software for metabolic flux analysis from ¹³C-glucose experiments. *BMC Bioinformatics.* 6, 209.
- Zamboni, N., Fendt, S.M., Rühl, M., Sauer, U., 2009. ¹³C-based metabolic flux analysis. *Nat. Protoc.* 4, 878–892.
- Zhang, H.H., Zhao, Z.F., Chen, S.N., Kang, P.L., Wang, Y., Feng, J., Jia, J.Y., Yan, M.M., Wang, Y., Xu, L., 2018. *Paracoccus versutus* KS293 adaptation to aerobic and anaerobic denitrification: Insights from nitrogen removal, functional gene abundance, and proteomic profiling analysis. *Bioresour. Technol.* 260, 321–328.
- Zhao, B., He, Y.L., Hughes, J., Zhang, X.F., 2010. Heterotrophic nitrogen removal by a newly isolated *Acinetobacter calcoaceticus* HNR. *Bioresour. Technol.* 101, 5194–5200.
- Zhou, Z.M., Takaya, N., Sakairi, M.A.C., Shoun, H., 2001. Oxygen requirement for denitrification by the fungus *Fusarium oxysporum*. *Arch. Microbiol.* 175, 19–25.